

Supplementary data

Combined Epitaxial Self-Assembly of the Block Copolymer Lamellae on Hexagonal Prepattern within Microgroove

Hyunjung Jung,^a Sanghoon Woo,^a Sungmin Park,^b Sumi Lee,^c Minhyuk Kang,^c
Youngson Choe,^d Jeong Gon Son,^e Du Yeol Ryu,^b June Huh^{*a} and Joona Bang^{*a}

^a Department of Chemical and Biological Engineering, Korea University, Seoul 136-713, Republic of Korea.

^b Department of Chemical and Biomolecular Engineering, Yonsei University, Seoul 120-749, Republic of Korea.

^c LCD R & D Center, Samsung Electronics San#24 Nongseo-dong, Giheung-gu, Yongin-city, Gyeonggi-do 446-711, Republic of Korea.

^d Department of Chemical Engineering, Pusan National University, Kumjeong-ku, Busan 609-735, Republic of Korea.

^e Photo-Electronic Hybrids Research Center, Korea Institute of Science and Technology (KIST), Seoul 136-791, Republic of Korea.

Received

First published on the web

DOI:

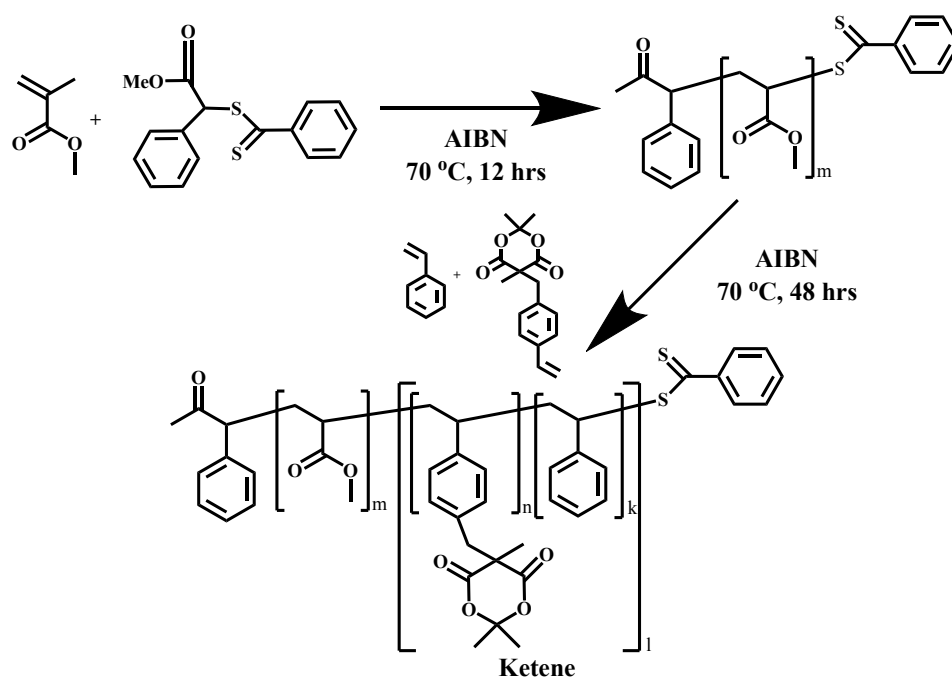


Fig. S1. Synthesis of crosslinkable PS-*b*-PMMA BCP containing the Meldrum's acid based monomer.

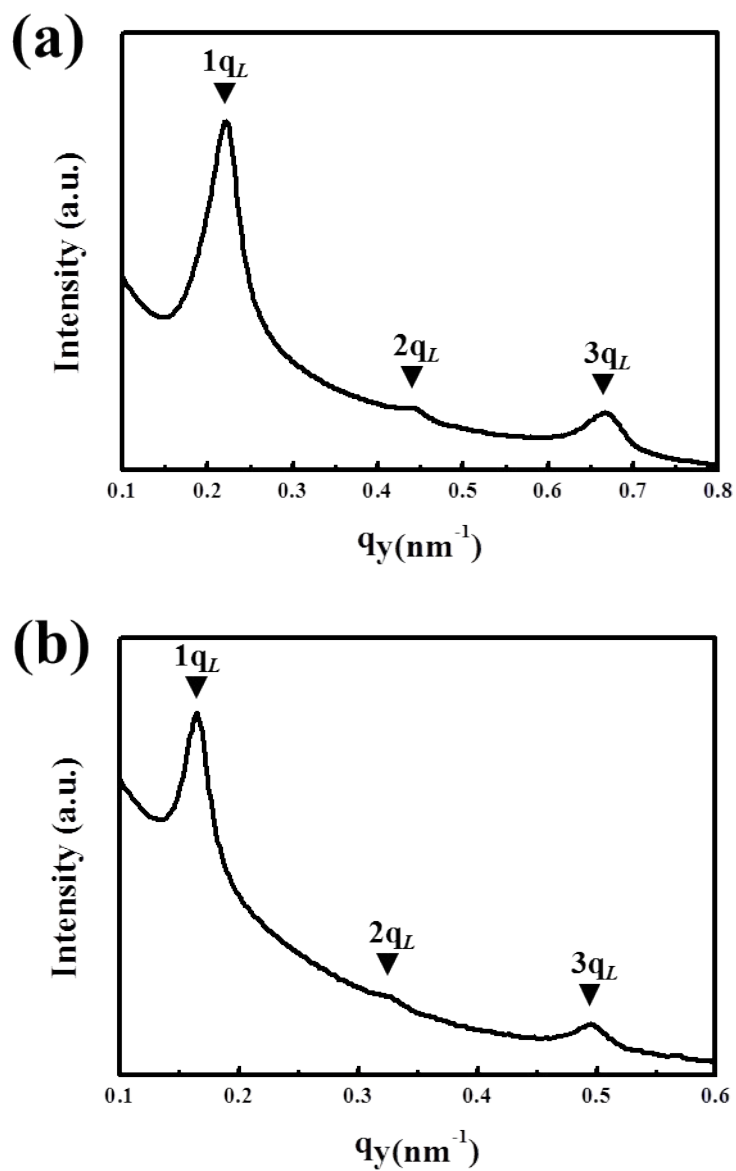


Fig. S2. SAXS traces illustrating the lamellar-forming PS-*b*-PMMA BCPs with (a) $M_n = 51 \text{ kg/mol}$ and (b) $M_n = 75 \text{ kg/mol}$.

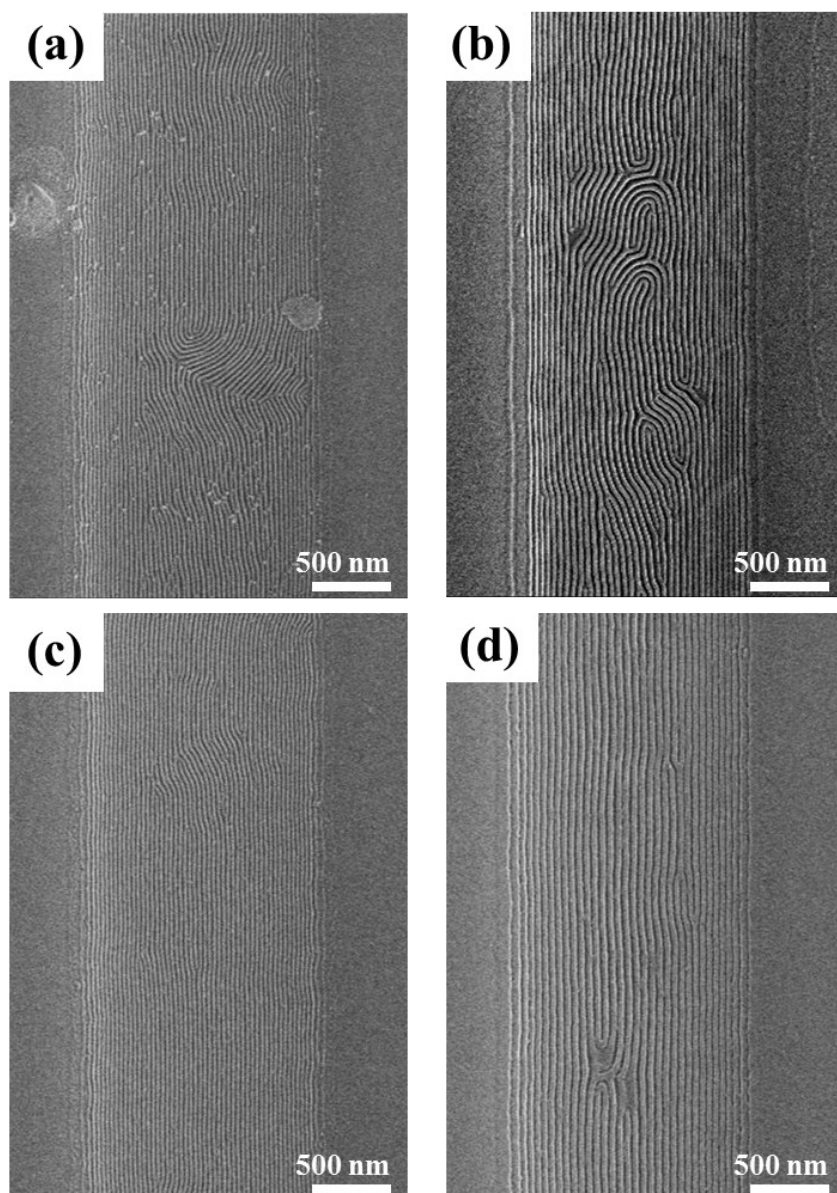


Fig. S3. SEM images of lamellar morphologies assembled within the 1.5- μm wide microgrooves. (a) and (b) correspond to SEM images for the PS-*b*-PMMA lamellae with $M_n = 51$ kg/mol and 75 kg/mol on the hexagonal prepatterns, respectively and (c) and (d) correspond to SEM images for the PS-*b*-PMMA lamellae with $M_n = 51$ kg/mol and 75 kg/mol on the neutral layers, respectively. They are larger area images of Figures 2(a)-(d).

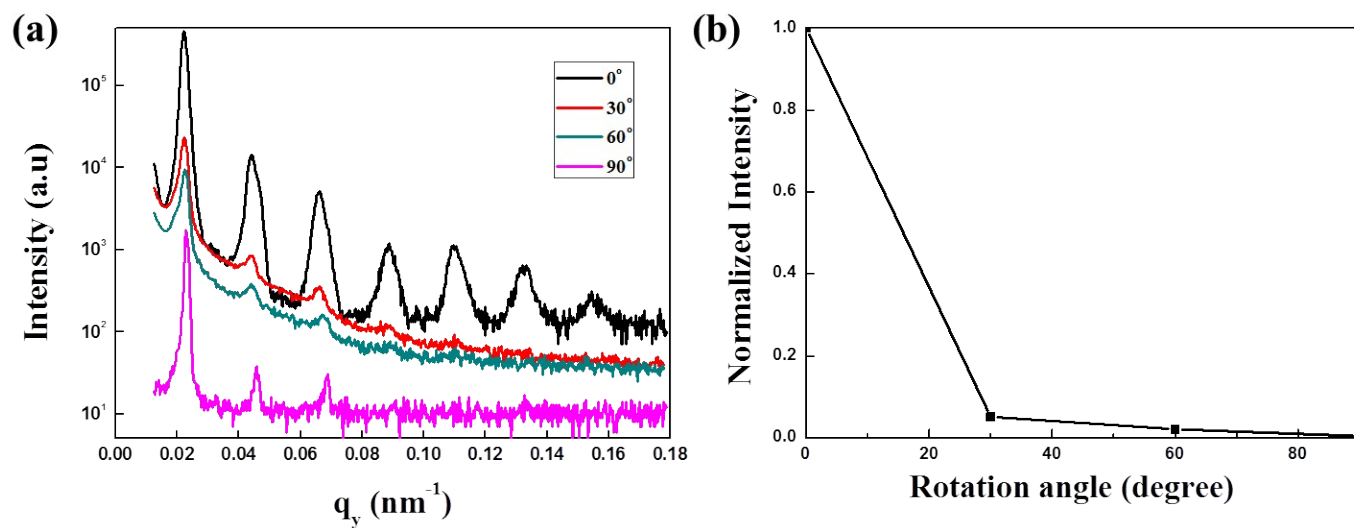


Fig. S4. (a) GISAXS intensity profiles of sample in Fig. 2a as a function of the scattering vector, q . During the measurement, the sample was rotated to adjust the beam direction as 0° , 30° , 60° , and 90° , with respect to the lamellar alignment. (b) Normalized intensity of first-order peaks in (a) as a function of sample rotating angle with respect to the incident beam direction. The GISAXS measurement was carried out at the 9A beamline at the Pohang Accelerator Laboratory (PAL), Korea.

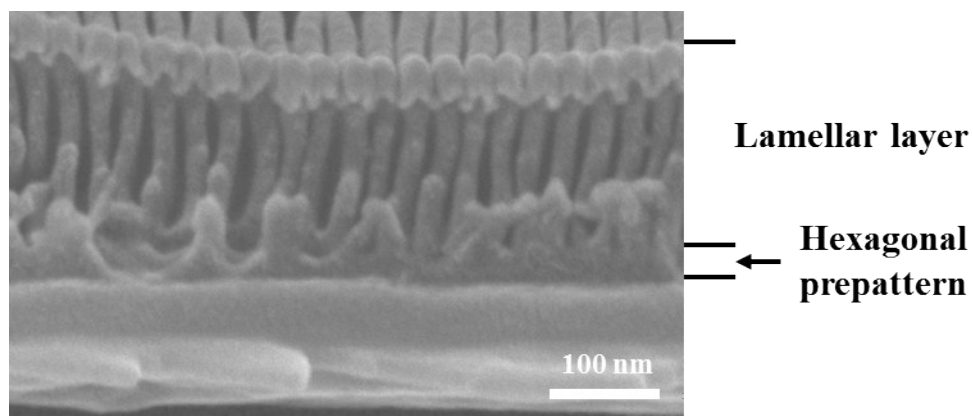


Fig. S5. Cross-sectional view of SEM image for PS-*b*-PMMA lamellae with $M_n = 51$ kg/mol assembled on the hexagonal prepatterns within the 1.5- μm wide microgrooves.

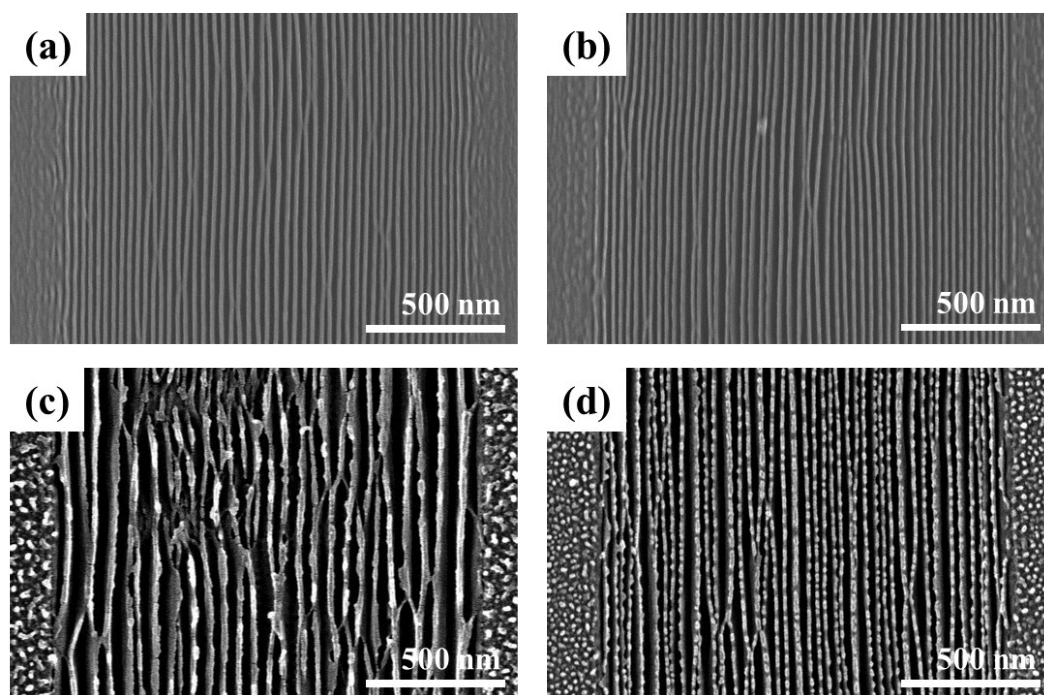


Fig. S6. Top-view of SEM images for PS-*b*-PMMA lamellae with $M_n = 51$ kg/mol assembled on the hexagonal prepatterns within the 1.5- μ m wide microgrooves with different RIE conditions (Ar (3 sccm)/O₂ (15 sccm) by a RF power of 20 W at 0.1 torr). (a), (b), (c), and (d) correspond to the etching time of 10 sec, 15, sec, 30 sec, and 60 sec, respectively, which lead to the thickness of residual lamellar layers as 140 nm, 130 nm, 40 nm, and 3 nm, respectively.

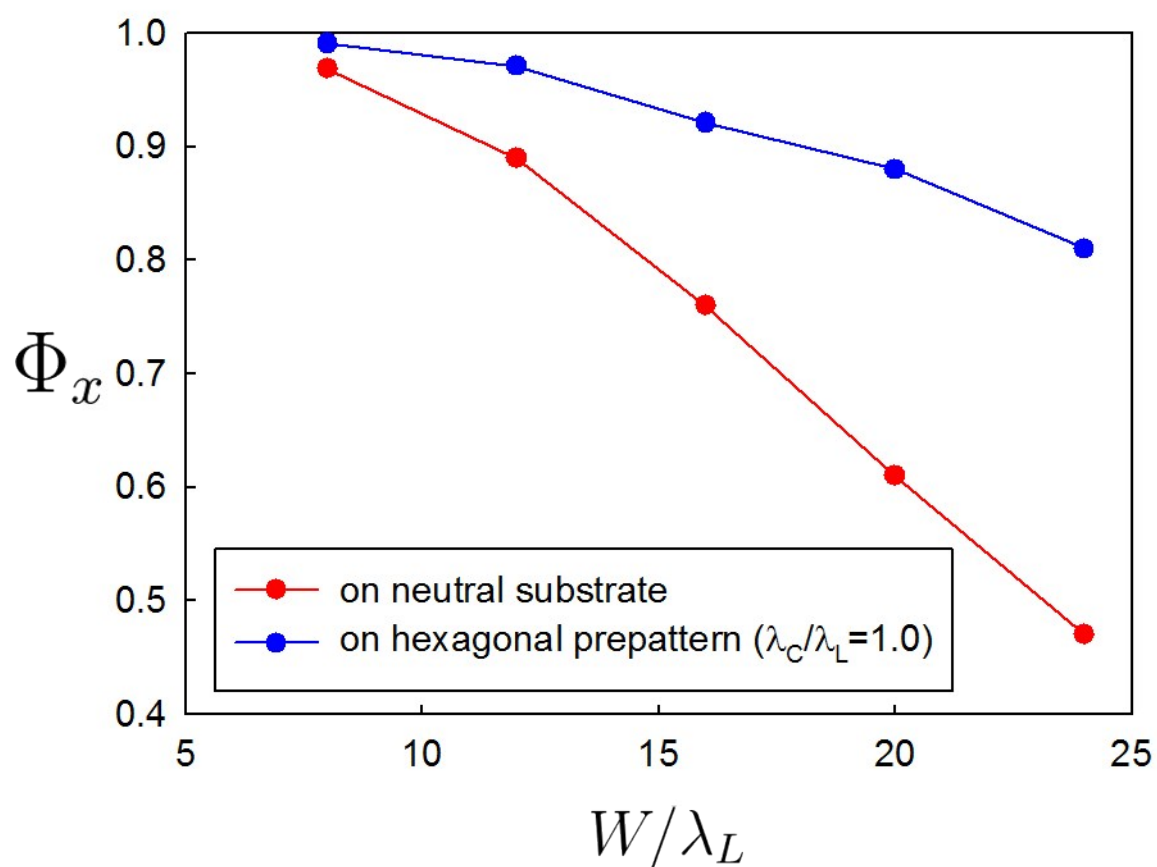


Fig. S7. The degree of alignment Φ_x as a function of trench width W for lamellae on the neutral substrate and on the hexagonal prepattern ($\lambda_C/\lambda_L=1.0$).